

Mutual Context Network for Jointly Estimating Egocentric Gaze and Actions

Yifei Huang, Zhenqiang Li, Yoichi Sato
The University of Tokyo
Tokyo, Japan
{hyf, lzq, ysato}@iis.u-tokyo.ac.jp

Minjie Cai
Hunan University
Changsha, China
cai-mj@iis.u-tokyo.ac.jp

Abstract

In this work, we address two coupled tasks of gaze prediction and action recognition in egocentric videos by exploring their mutual context. Our assumption is that in the procedure of performing a manipulation task, what a person is doing determines where the person is looking at, and the gaze point reveals gaze and non-gaze regions which contain important and complementary information about the undergoing action. We propose a novel mutual context network (MCN) that jointly learns action-dependent gaze prediction and gaze-guided action recognition in an end-to-end manner. Experiments on public egocentric video datasets demonstrate that our MCN achieves state-of-the-art performance of both gaze prediction and action recognition.

1. Introduction

The popularity of wearable cameras in recent years is accompanied by a large number of first-person view videos, or often called egocentric videos, that record persons' daily interactions with their surrounding environments. The demand for automatic analysis of egocentric videos has promoted various egocentric vision techniques [1] such as egocentric video hyper-lapse [18, 34] and video summarization [24, 49]. In particular, the task of understanding what a person is doing and where a person is looking at have attracted great interests from researchers. The former task is often called *egocentric action recognition* [23, 25] and the latter is called *egocentric gaze prediction* [21, 54, 11]. Although the two tasks have been studied extensively in the past years, few works have focused on the relationships between the two tasks which are in fact deeply related.

This work aims to jointly model the two coupled tasks of gaze prediction and action recognition in egocentric videos. Previous works have studied how gaze could be used for action recognition [6, 22]. They tried to model human gaze in egocentric videos and use estimated gaze points for removing unrelated background information, in order to improve action recognition. While the guidance of gaze for action

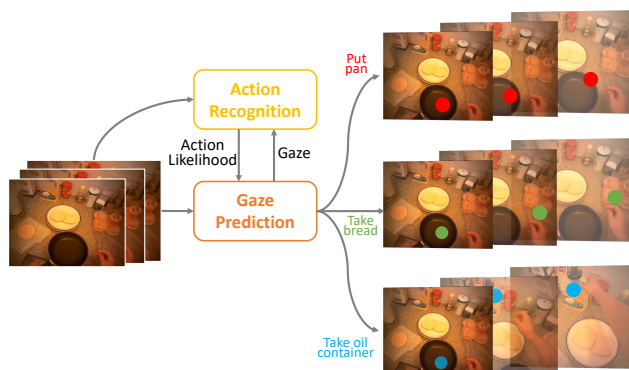


Figure 1. Different actions in egocentric videos will result in different gaze patterns. Our method leverages this observation and explicitly uses action likelihood as a prior for egocentric gaze prediction.

recognition has been studied, gaze itself was simply modeled as a saliency prediction problem, and no effort has been seen to explicitly explore the influence of actions for gaze prediction.

In an egocentric video, background regions are often cluttered and may contain multiple salient regions. Therefore, it would be difficult for a saliency-based model to predict gaze reliably without additional information about the location of gaze. It has been studied by psychologists that an action performed by a person implicitly affects where the person is looking [43, 45]. For example, to take a knife from a table, a person always moves his/her focus onto the knife and then keeps fixating on the knife before grasping it. Therefore, we argue that for better modeling of gaze and actions in egocentric videos, not only the gaze-guided action recognition (gaze context for actions) but also the action-dependent gaze prediction (action context for gaze) should be jointly considered.

In this paper, we propose a mutual context network (MCN) that jointly predicts human gaze and recognizes actions in egocentric videos with consideration of mutual context between the two coupled tasks. The proposed model MCN takes a video sequence as input and outputs action

likelihood as well as a gaze probability map for each frame. Two novel modules are developed within the model to leverage the context from the predicted actions and gaze probability maps respectively. The first module called the action-dependent gaze prediction module takes the predicted action likelihood as input and produces a set of convolutional kernels that are relevant to the action being performed. The generated action kernels are then used to convolve input feature maps for locating action-related regions. The second module called the gaze-guided action recognition module uses the estimated gaze point as a guideline to spatially aggregate the input features for action recognition. Rather than only using the region around the gaze point as in previous work, the features are aggregated both in the gaze region and the non-gaze region separately and then used as input to the gaze-guided action recognition module, while the relative importance of the two regions is learned automatically during training.

Our main contributions are summarized as follows:

- We propose a novel MCN for both egocentric gaze prediction and action recognition that leverages the mutual context between the two tasks.
- We propose a novel action-dependent gaze prediction module that explicitly utilizes information from the estimated action for gaze prediction. This is done by generating convolution kernels for gaze prediction adaptively with the estimated action.
- Our proposed MCN achieves state-of-the-art performance in both gaze prediction and action recognition and is able to learn action-dependent gaze patterns. The code will be made publicly available.

2. Related works

2.1. Egocentric gaze prediction

Predicting gaze in an egocentric video can benefit a diverse range of applications such as joint attention discovery [29, 14, 10], action recognition [6], human computer interaction [15, 19, 7], and video summarization [49]. Despite the correlation between gaze and saliency [30], previous works have revealed the need for additional cues for predicting gaze in egocentric videos [51, 52, 21, 54, 11]. Li *et al.* [21] used head motion and hand cues in a graphical model for gaze prediction. However, the pre-defined egocentric cues may limit the generalization ability of their model. Huang *et al.* [11] proposed a hybrid deep model which incorporates task-dependent gaze shift patterns in addition to a bottom-up saliency-based model. However, they did not consider the differences in gaze patterns with respect to different actions.

In this work, we explicitly leverage the contextual information from the performed actions for gaze prediction by

using the predicted action likelihood. To the best of our knowledge, this is the first work to explore the influence of actions for egocentric gaze prediction.

2.2. Egocentric action recognition

Egocentric action recognition is one of the focused fields in egocentric vision and has been studied extensively in recent years [41, 32, 27, 26, 23, 33, 53, 25, 39, 42]. Kitani *et al.* [17] used global motion to discover different egocentric actions in an unsupervised manner. Fathi *et al.* [5] adopted a graphical model to recognize actions in relation to objects and head/hand motion. Ryoo *et al.* [36] proposed a novel pooling method for action recognition. Ma *et al.* [25] proposed a comprehensive deep model for recognizing objects and actions jointly. Singh *et al.* [39] used additional inputs like hand masks to improve action recognition performance. Different from previous works, our method recognizes actions with the contextual information from gaze by modeling actions and gaze in a unified framework.

2.3. Gaze and actions

Human gaze and actions are deeply correlated in egocentric videos, and the use of gaze has been proved to be beneficial for action recognition [6, 37]. However, little work has been done on the joint modeling of egocentric gaze prediction and action recognition. Extended from [6], Li *et al.* [22] proposed a deep model for jointly modeling gaze and actions. They modeled the probabilistic nature of gaze and used the estimated gaze for better action recognition. However, their work did not explicitly consider the contextual information from actions for gaze prediction. Gaze prediction will be less reliable without the contextual information of actions.

In this work, we leverage the mutual context of gaze and actions in our proposed model, in the form of using action likelihood as a conditional input to predict gaze, and simultaneously using gaze as a guidance for action recognition. By explicitly exploring such mutual context, our model achieves state of the art performance in both gaze prediction and action recognition.

3. Method

In this section, we first introduce the basic models for gaze prediction and action recognition for clarity of illustration. We then explain our proposed MCN followed by details of each of its modules. Lastly, we provide details of the model architecture and training at the end of this section.

3.1. Basic models

In egocentric videos, the point of gaze is conventionally represented as a 2D isotropic Gaussian [21, 22]. Since the 2D Gaussian is represented as a one channel image with the same size of the original image, one direct

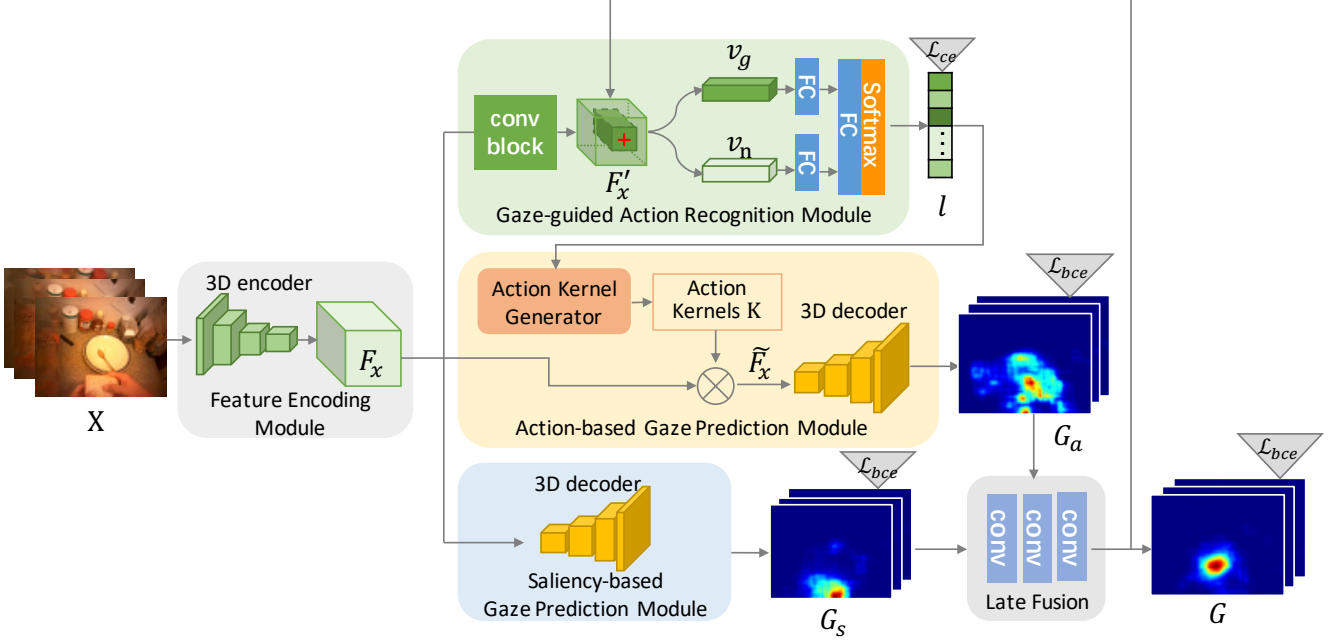


Figure 2. Our proposed mutual context network (MCN) contains 5 sub-modules: the feature encoding module which encodes input video frames into feature maps F_x , the gaze-guided action recognition module which uses gaze as a guideline to recognize actions, the action-based gaze prediction module which takes predicted action likelihood l as input and outputs a action-dependent gaze probability map G_a , the saliency-based gaze prediction module which outputs a saliency map G_s , and finally the late fusion module to get the final gaze probability map G .

way to predict gaze is to use an encoder-decoder network [9, 28, 55, 47, 20] which takes a video frame as input and outputs a gaze probability map. To take motion information into account, the encoder-decoder network could adopt a two-stream network [11] or 3D convolution [54]. Formally speaking, denote $X = \{x_1, x_2, \dots, x_n\}$ as the input video frames and $G = \{g_1, g_2, \dots, g_n\}$ as gaze probability maps, a basic gaze prediction model can be expressed as:

$$F_x = \text{Encoder}(X), \quad (1)$$

$$G = \text{Decoder}(F_x), \quad (2)$$

in which F_x denotes the encoded feature maps of the input video X .

As for egocentric action recognition, a standard approach is to adopt one of the state-of-the-art action recognition models [3, 38, 48, 44, 40] and finetune on egocentric videos. The model outputs the likelihood of action $l \in \mathbb{R}^c$ as a vector whose dimension is identical with the number of action categories c .

3.2. Our proposed MCN

3.2.1 Overview

When performing a task, especially a hand manipulation task, human gaze and actions of hand-object interaction are tightly related. While image region around a person's gaze

point explicitly reveals important information about the undergoing action, the action performed by the person implicitly affects where the person is looking. In this work, we propose a mutual context network that uses the estimated action to predict gaze point and uses gaze as a guidance for action recognition.

Figure 2 depicts the architecture of our MCN. The input video frames are first encoded as feature maps F_x by the feature encoding module, which are then used as input to the following modules. One of the key components in our model is the action-dependent gaze prediction module that learns to predict gaze using the predicted action likelihood as a conditional input. As complementary information for gaze prediction, we also obtain a saliency map with the saliency-based gaze prediction module. The outputs from the two modules are then fused by the late fusion module to get the final gaze probability map. Another key component in our MCN is the gaze-guided action module which takes the predicted gaze as guidance to selectively filter the input features for action recognition. The output of action likelihood is then used as conditional input to the action-dependent gaze prediction module, thus a loop of mutual context is constructed.

3.2.2 Feature encoding module

We adopt the first four convolutional blocks of the 3D convolution network I3D [3] for feature encoding from a given input set of RGB frames. Note that, two stream I3D networks with both RGB frames and dense optical flow could be used alternatively at the expense of higher computational cost. With the 3D encoder, the output feature map F_x is with the size of (c, t, h, w) , where c is the number of channels, t is the temporal dimension, and (h, w) are the spatial height and width.

3.2.3 Saliency-based gaze prediction module

Image regions with high saliency tend to attract human attention. For instance, regions with unique and distinguishing features such as a moving object or high contrast of brightness are more likely to be looked at than other regions. Therefore, we use a saliency-based gaze prediction module to learn the image regions that are more likely to draw human attention. For this, we use a 3D decoder that takes the encoded feature map F_x as input and outputs a series of gaze probability maps G_s with each pixel value within the range of $[0, 1]$. While this bottom-up approach provides information of salient regions in the image, it is not sufficient to reliably identify the attended region when multiple salient regions exist, which is common in egocentric video.

3.2.4 Action-dependent gaze prediction module

As different actions are associated with different objects and motion, the gaze patterns when performing different actions is different. It is necessary for the gaze prediction module to leverage action information for more reliable gaze prediction. To this end, inspired by [50, 4], we use the output of the gaze guided action recognition module to generate a group of convolutional kernels that are used to identify the regions relevant to the performed action. The generated action kernels are then used to convolve with the input features in order to locate the action-related regions. Finally, gaze probability maps that have the same size with input frames are generated with a decoder consisting of deconvolutional layers.

More formally, given action likelihood $l \in \mathbb{R}^c$ estimated by the action recognition module and the input feature maps $F_x \in \mathbb{R}^{c,t,w,h}$ with c channels (t and w, h are temporal and spatial dimension), the gaze probability map G_a is generated through the following procedure:

$$K = G_k(l) \quad (3)$$

$$\tilde{F}_x = K \otimes F_x \quad (4)$$

$$G_a = \text{Decoder}(\tilde{F}_x) \quad (5)$$

where G_k is the kernel generator, $K \in \mathbb{R}^{k,c,k_t,k_w,k_h}$ is a group of k kernels, and $\tilde{F}_x \in \mathbb{R}^{k,t,w,h}$ is the filtered feature maps. \otimes denotes the operator of convolution. The kernel generator contains one fully connected layer and two convolutional layers. The output of the first fully connected layer is first reshaped into size (k_t, k_w, k_h) and then forwarded to the following convolution layers.

We also adopt the saliency-based gaze prediction module which can be seen as a complementary to the action-based gaze prediction module. Finally we use a late fusion module to combine the outputs G_s and G_a from the previous modules:

$$G = LF(G_s, G_a) \quad (6)$$

Late fusion technique has been proved to be effective in previous work of gaze prediction [11]. Following previous work [54, 21, 11], we take the spatial location with maximum likelihood on G as the predicted gaze point.

3.2.5 Gaze-guided action recognition module

Here we describe the gaze-guided action recognition module in our MCN that uses the predicted gaze point as a guideline to exploit discriminative features for action recognition. Previous works [6, 22] mostly used gaze as a filter to remove features of image regions distant to the gaze point. However, focusing only on the region around the gaze point might lose important information about the action. We observed that when performing certain actions such as “put an object”, the person may fixate on the table on which to place the object instead of looking at the object in hand which contains critical information about the action. Therefore, we think that while the gaze region is important, the region outside the gaze (non-gaze region) might also contain complementary information about the action. In this work, we develop a two-way pooling structure to aggregate features in the gaze and non-gaze regions separately and use both as input for action recognition.

As shown in Figure 2, we first add another convolutional block on the F_x from feature encoding module to encode more abstract features F'_x . With the predicted gaze point, we locate the corresponding spatial location (x, y) on the feature map and first average F'_x on the time dimension. Then we split the feature map into two parts: gaze region and non-gaze region. Gaze region on a feature map (dark green region of F'_x in the figure) is the locations whose spatial positions are within range $([x-r, x+r], [y-r, y+r])$, and non-gaze region is the left-out region (light green region of F'_x in the figure). We pool the two regions separately on the spatial dimensions, generating two feature vectors v_g

and v_n :

$$v_g[c] = \frac{\sum_{i=x-r}^{x+r} \sum_{j=y-r}^{y+r} \bar{F}'_x(c, i, j)}{4r^2} \quad (7)$$

$$v_n[c] = \frac{\sum_i \sum_j \bar{F}'_x(c, i, j) - 4r^2 v_g[c]}{h \times w - 4r^2}, \quad (8)$$

where $\bar{F}'_x(c, i, j)$ denotes the c -th channel and position (i, j) of the time averaged feature map F'_x , $v[c]$ denotes the c -th element in v .

The pooled feature vectors v_g and v_n are feed into two separated fully connected (FC) layers, and the outputs are concatenated and forwarded into the final FC layer for predicting the action likelihood l :

$$v'_g \in \mathbb{R}^s = W_g v_g + b_g \quad (9)$$

$$v'_n \in \mathbb{R}^{s/2} = W_n v_n + b_n \quad (10)$$

$$l = \text{Softmax}(W_p \{v'_g; v'_n\} + b_p) \quad (11)$$

Here W_g , W_n , W_p and b_g , b_n , b_p are the learned weights and bias correspondingly. $\{;\}$ denotes channel-wise concatenation. We set the output size of v'_g to be s and v'_n to be $\frac{s}{2}$ since the modeling of non-gaze region is empirically simpler than that of the gaze region, so we limit its vector size to prevent over-fitting.

3.3. Implementation and training details

The whole framework is implemented using Pytorch framework [31]. The feature encoding module is identical to the first 4 convolutional blocks of the I3D [3] network without the last pooling layer. With our input of 24 stacked images of size 240×320 , the output of feature encoding module is of size $c = 832, t = 6, h = 14, w = 14$. The decoder contains a set of 4 transposed convolution layers, with kernel sizes 4, 4, (3, 4, 4), (3, 4, 4), and stride 2, 2, (1, 2, 2), (1, 2, 2) respectively. Padding 1 is added on all layers. Each layer is followed by batch normalization and ReLU activation. We add another convolution layer with kernel size 1 and a sigmoid layer on top of the decoder for outputting values within $[0, 1]$. The kernel decoder takes the input vector $l \in \mathbb{R}^n$ where n is the number of action categories, and firstly encoded to latent size of \mathbb{R}^{2880} and reshaped into (64, 5, 3, 3). The two convolutional layers output channels 256 and 832, with kernel size 3, stride 1 and padding 1. The output size of the action kernel generator is $(k, k_t, k_w, k_h) = (64, 3, 5, 5)$. For the gaze guided action recognition module, the convolution block is identical to the 5-th convolution block of the I3D network. We set $r = 1$ and $s = 512$.

For training the whole network, we first train the base I3D network for action recognition by using SGD and saliency-based gaze prediction module by using Adam optimizer [16] for gaze prediction. All input images we used

are resized as 320×240 . The base I3D weights are initialized from weights pretrained on kinetics dataset [13]. The results of the base I3D network are used as initialization of the remaining modules. We then use the result of action recognition to train action-based gaze prediction module and use the initialized gaze prediction results for training gaze-guided action recognition module. We do not alternatively update the modules since no performance improvement was observed in our preliminary experiments. We use cross entropy loss for action recognition and binary cross entropy loss for gaze prediction. We apply a Gaussian with $\sigma = 18$ on the gaze point for generating ground truth images for gaze prediction. For training action recognition modules, we first use learning rate of 0.01 and decay the learning rate by a factor of 10 when testing accuracy saturates. For training gaze prediction modules we fix the learning rate to be 10^{-7} . We random crop images into 224×224 , random flip with probability 0.5 for data augmentation when training. Ground truth gaze images perform the same data augmentation. When testing, we send both the images and their flipped version and report the averaged performance.

4. Experiments

4.1. Dataset

Our experiments are conducted on the public EGTEA [22] dataset. The dataset contains 29 hours of egocentric videos with the resolution of 1280×960 and 24 fps, taken from 86 unique sessions with 32 subjects performing meal preparation tasks in a kitchen environment. This dataset also contains the previous GTEA Gaze+ dataset [23] as a subset. Fine-grained annotations of 106 action classes are provided together with measured ground truth gaze points on all frames. Following [22], we use the first split (8299 training and 2022 testing instances) of the dataset to evaluate the performance of gaze prediction and action recognition.

4.2. Performance comparison

We compare different methods on both tasks of gaze prediction and action recognition. For gaze prediction, we adopt two commonly used evaluation metrics: AAE (Average Angular Error) [35] and AUC (Area under Curve) [2]. For action recognition, we use classification accuracy as the evaluation metric.

4.2.1 Gaze prediction results

We compare our method with the following baselines:

- Traditional saliency prediction methods: **GBVS** [8] and **Itti's model** [12]. Both methods are the representative methods for saliency prediction in images.

Method	AAE (deg)	AUC
GBVS [8]	10.227	0.707
Itti <i>et al.</i> [12]	10.023	0.717
Li <i>et al.</i> [22]	8.578	0.870
SALICON [9]	7.564	0.905
Huang <i>et al.</i> [11]	6.264	0.910
DFG [54]	6.301	0.923
Saliency-based	6.361	0.922
Action-based	6.195	0.928
Action-based + GT action	6.037	0.927
Our full MCN	5.788	0.932

Table 1. Comparison of gaze prediction performance on EGTEA dataset. Results of previous methods are placed on top. Results of the subsets of our full MCN and our full MCN trained with ground truth action labels are places on the bottom. Lower AAE and higher AUC indicate better performance.

- FCN-based saliency prediction: We re-implement the **SALICON** [9] model and train on same dataset with gaze as ground truth heatmap.
- Egocentric gaze prediction methods: We also compare with three egocentric gaze prediction methods most related to our work: coarse gaze prediction method (**Li *et al.* [22]**), the GAN-based method (**DFG [54]**), and the attention transition-based method (**Huang *et al.* [11]**). Since [22] only outputs a coarse gaze prediction map (of resolution 7×7), we resize their output using bi-linear interpolation. For [11] fixation states are directly determined from the ground truth gaze data, instead of being estimated from optical flow images.
- Subsets of our full MCN: We also conduct ablation study using subsets of our full model. These include the saliency-based gaze prediction module (**Saliency-based**), the action-dependent gaze prediction module (**Action-based**). In addition, we also test the action-dependent gaze prediction module with ground truth action labels (**Action-based + GT action**).

Table 3 shows the quantitative comparison of different methods on gaze prediction performance. Although our saliency-based gaze prediction module alone cannot get preferable performances against state-of-the-art gaze prediction methods of [54] and [11], our action-based gaze prediction module clearly outperforms all previous methods. This strongly indicates the usefulness of actions in gaze prediction. Our full model even outperforms the action-based saliency prediction module, which demonstrates that an ideal gaze prediction method should consider information from both bottom-up visual saliency and top-down influence of actions. The superiority of encoder-decoder

Method	clip Acc (%)	Video Acc (%)
EgoIDT + Gaze* [23]	N/A	46.50
EgoConv + I3D [39]	N/A	48.93
I3D [3] †	46.42	49.79
I3D [3] + Gaze* †	46.77	51.21
Li <i>et al.</i> †[22]	47.71	53.30
MCN (gaze region only)	48.56	51.53
Our full MCN	51.42	53.70

Table 2. Quantitative comparison of action recognition of EGTEA Dataset. * indicates using measured human gaze as input and † indicates using dense optical flow as input.

based SALICON [9] over [22] reveals the importance of using decoder-based structure for fine-grained gaze prediction.

Comparing subsets of our MCN, the action-dependent module performs better than the saliency-based module and even better than the state-of-the-art methods, indicating the effectiveness of action information in gaze prediction. When feeding the action-based module with ground-truth action labels, the performance is further improved. The performance of our full MCN significantly improves by integrating the two sub-modules. This strongly indicates that the action-based gaze prediction module and the saliency-based gaze prediction module represent complementary information and should be jointly considered.

Qualitative results are shown in Figure 3. It can be seen that with the help of the action-based gaze prediction module, our full MCN can better locate the action, thus giving better gaze prediction results. For example, in the first row, our MCN successfully recognizes the action as “take paper towel”, thus finds the paper towel in the hand. Other baseline methods mostly focus on the stove or other salient regions. In the second row, while other methods are distracted by the plates and food on the counter, our MCN successfully locates the hand with dishrag on the bottom right corner and a part of the counter which will be cleaned in the next few frames. More interestingly as shown in the fourth row, the lettuce of ground-truth gaze fixation is placed on a cluttered kitchen table, which is challenging for other methods to locate. Still, our full MCN correctly predicts gaze on the lettuce with the help of context from the action “take lettuce”. Similar situations can be found in other rows of the figure.

4.2.2 Action recognition results

As for the task of action recognition, we compare our method with the following baselines:

- State-of-the-art action recognition models: **I3D** [3] is one of the state of the art models for action recognition.

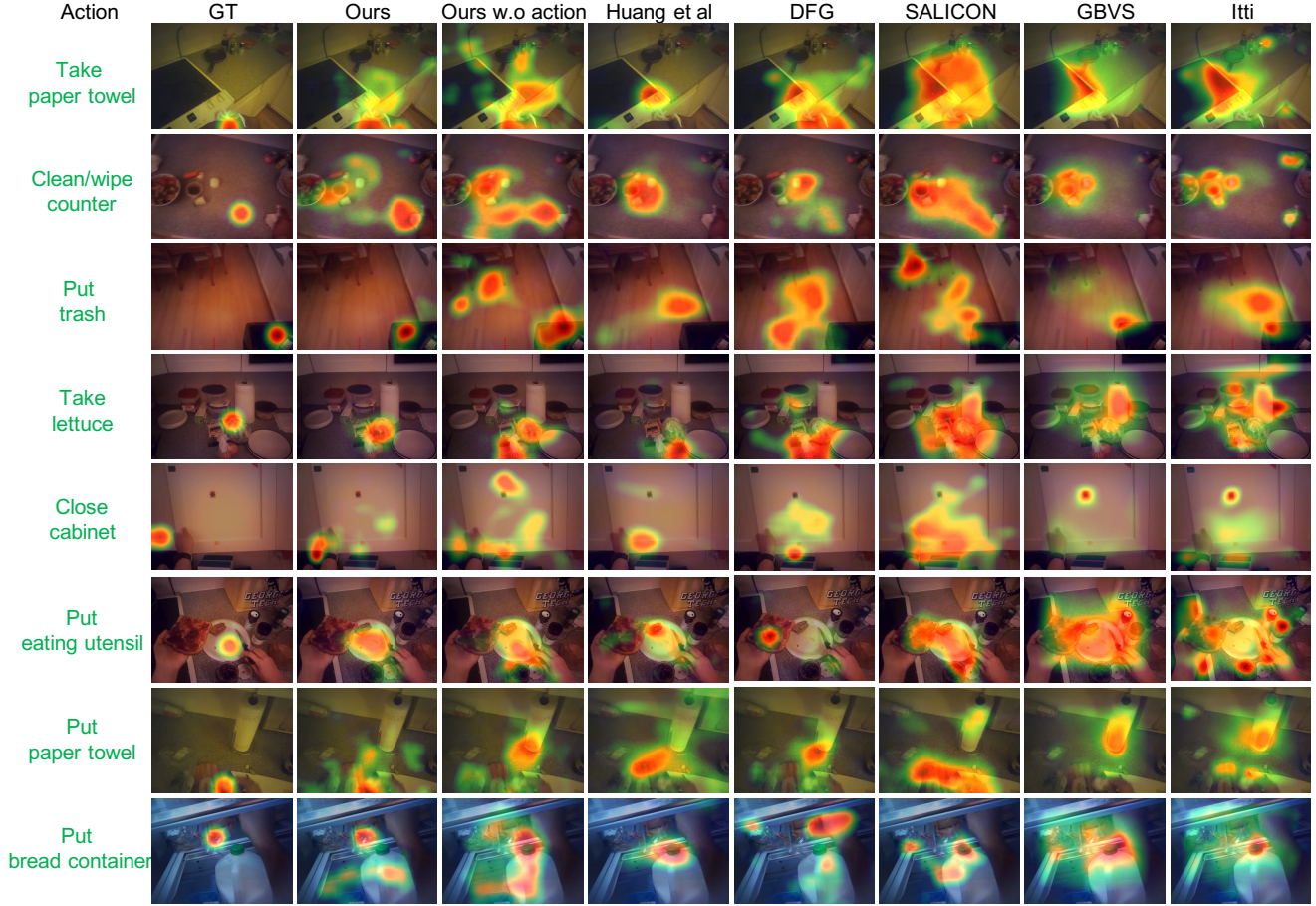


Figure 3. Qualitative visualizations of gaze prediction results. We show the output heatmap from our full MCN and several baselines. Ground truth action labels and gaze points (GT) are placed on the leftmost columns.

EgoConv+I3D [39] adds another stream which encodes rich egocentric cues together with base streams. We refer to [22] for the accuracy of these baseline methods.

- Methods using measured gaze: **I3D+Gaze** is to use a ground truth gaze point as a guideline to pool feature maps from the last convolution layer of the fifth convolutional block. **EgoIDT+Gaze** [23] is a traditional method which uses dense trajectories [46] selected by a ground truth gaze point for action recognition.
- State-of-the-art egocentric action recognition: **Li et al.** [22] uses a probabilistic modeling of gaze which generates a coarse gaze probability map as soft attention to perform weighted average on top I3D features.
- Baseline of our model: **Ours (gaze region)** is a baseline of our MCN that uses only the gaze region for pooling without using non-gaze regions. We use this baseline to validate the usefulness of information from the non-gaze regions.

Table 4 lists the action recognition accuracy of our model and baseline methods. Following [22], we report clip accuracy (24 frames) and video accuracy. I3D [3] outperforms previous methods using hand crafted features EgoIDT+Gaze [23] and EgoConv+I3D [39] which were designed for recognizing gross body motion. With the use of measured gaze, the performance of I3D+Gaze got slightly improved than I3D. Our MCN outperforms all previous methods in clip accuracy, and performs comparably with the state of the art method [22] on video accuracy, even without using optical flow as input. We also conduct ablation study and compare with our baseline that only uses gaze region for action recognition. The superiority of our MCN over the baseline validates our thought that the non-gaze regions contain supplementary information and should be jointly considered in action recognition.

We visualize the confusion matrix of all 106 action classes based on clip accuracy in Figure 4. To better show the results, we also visualize the confusion matrix of the top 20 frequent action classes in Figure 5. It can be seen that the action classes related to “cut” can be classified very

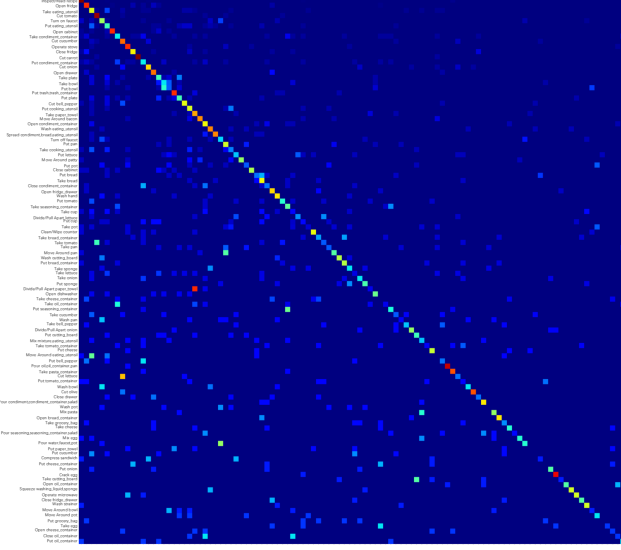


Figure 4. Confusion matrix of all 106 action classes based on clip accuracy. Mean accuracy is 51.42%.

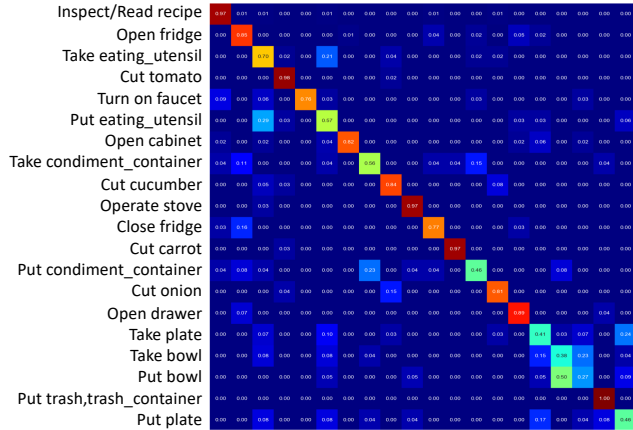


Figure 5. Confusion matrix of the top 20 frequent action classes.

well. The misclassification mainly comes from the action classes of “put” and “take” when holding the same object.

4.3. Examination of action-based gaze prediction module

We further demonstrate that our action-based gaze prediction module is able to learn meaningful gaze patterns relevant to different actions. Intuitively, the gaze patterns for similar actions should also be similar. For example, for the action “take bowl”, the gaze prediction performance should not decrease obviously if we use a label of “take plate” as input to the action-based gaze prediction module, but should decline sharply if it is given the label of “cut tomato” as input. Thus we conduct a new experiment on the top 20 frequent actions in test set of EGTEA dataset to examine our action-based gaze prediction module. We feed the module with action likelihood representing each of the 20 ac-



Figure 6. Affinity matrix of the top 20 frequent actions in EGTEA dataset. Actions are re-ordered for the ease of viewing. Each row of the matrix represent the affinity score of one action against all the 20 actions. Blue indicates higher affinity between corresponding actions.

tion classes and examine how gaze prediction performance (AAE score) varies when the module is tested on each of these actions. For example, we feed the action-based gaze prediction module with the action likelihood of “take plate” and test the AAE scores on the videos of all 20 actions. As a result, we obtain a matrix of AAE scores with the size of 20×20 , denoted by M , in which $M_{i,j}$ is the AAE score of the action-based gaze module fed with the action likelihood of the i -th action and applied to the videos of the j -th action. We then compute an affinity matrix A with the following equation:

$$A_{i,j} = 1 - \frac{M_{i,j} - \min(M_{i,*})}{\max(M_{i,*}) - \min(M_{i,*})}, \quad (12)$$

where $A_{i,j}$ can be seen as the affinity score between the measured ground truth gaze pattern of the i -th action and the learned gaze pattern of the j -th action-specific gaze module. We normalize each number to have numeric range of $[0,1]$.

We visualize the affinity matrix in Figure 6. We can see from several dark blocks along the diagonal that there exist several groups of actions of which the learned gaze patterns are similar to each other, for example, the action group of “put” and the action group of “cut”. The obtained affinity matrix is actually consistent with our common sense of these actions. For the action group of “put”, persons tend to fixate on a table which is often the destination of placement. For the action group of “cut”, the gaze is often fixated on a knife. More importantly, the results show that our action-based gaze prediction module has learned meaningful action-based gaze patterns and can be used to study the similarity between different actions from the perspective of human attention.

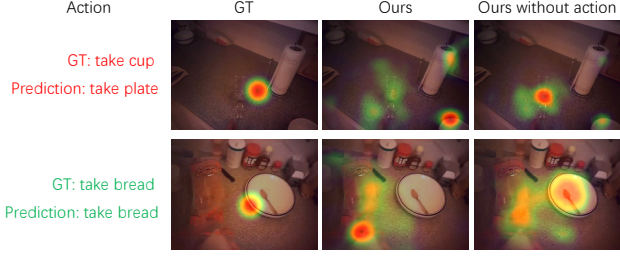


Figure 7. Failure cases of our MCN on gaze prediction. In the first row, failed action recognition misleads gaze prediction. In the second row, although the action recognition is correct, the camera wearer shifts the gaze fixation onto the region of future destination when he/she has already finished an action of grabbing the bread.

4.4. Failure cases and discussion

Here we discuss several failure cases we faced. One failure case comes from the inaccuracy of action recognition. As shown in the first row of Figure 7, although we use a late fusion module to fuse the outputs of the sub-modules, our model may fail when action recognition gives a wrong result. Still, the impact from failed action recognition is limited in our model. Our MCN can still outperform other methods: among all the testing data, our model achieves AAE score of 6.110 when action recognition fails, and AAE score of 5.921 when action recognition is correct.

Another failure case comes from the circumstances where a person begins to shift the gaze fixation between consecutive actions. An example is shown in the second row of Figure 7. After grabbing the bread, instead of keeping fixation on the bread, the person’s attention goes to the plate on which he’s planning to put the bread. Other than increasing the action recognition accuracy, this reveals the necessity of taking attention transition [11] into consideration for our current gaze prediction model.

We give more detailed analysis on how the action recognition results influence gaze prediction performance. In Figure 8 (a), we show the classification accuracy of the top 20 frequent action classes. In (b), we show the Average Angular Error (AAE) of the saliency-based gaze prediction module only (noted as AAE_s) and our full model (noted as AAE_f). The difference of AAE_s and AAE_f , noted as AAE_{diff} , is shown in (c) using the following equation:

$$AAE_{diff} = AAE_s - AAE_f \quad (13)$$

such that higher AAE_{diff} indicates larger performance gain is achieved by incorporating the action-based gaze prediction module.

From Figure 8, it can be seen that for actions with classification accuracy higher than 90% (actions 1, 4, 10, 12), either AAE score is good and below 5.0 (actions 4, 10, 12) or obvious gain of gaze prediction performance is obtained

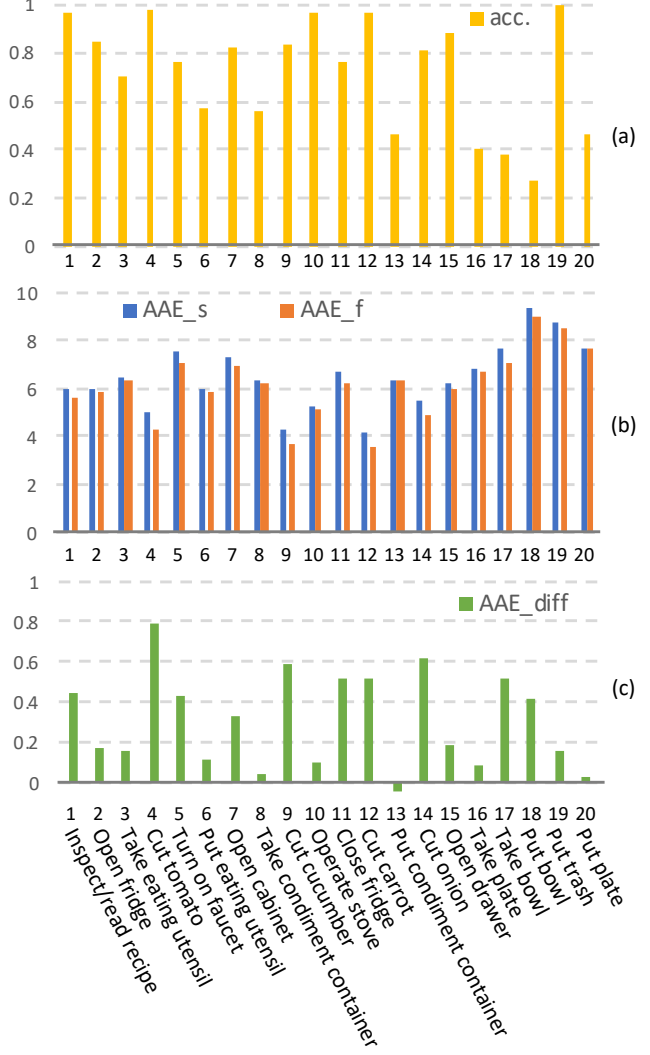


Figure 8. Performance analysis of gaze prediction and action recognition based on the the top 20 frequent action classes on EGTEA dataset. (a) Action recognition accuracy. (b) Gaze prediction AAE performance of the saliency-based gaze prediction module only (AAE_s) and our full model (AAE_f). Lower AAE indicates better performance. (c) represents the difference of the two AAE scores in (b). Larger values in (c) indicate larger gain the full MCN get from the action-based gaze prediction module.

(actions 1, 4, 12). This supports our statement that the information of actions can help gaze prediction.

One exception is action 19: “Put trash”. While classification accuracy of this action is high, the gaze prediction performance is low and no obvious gain is obtained. We think the reason might be due to the large head motion in this action, which limits the performance of gaze prediction.

Inversely, for the actions with classification accuracy lower than 50% (actions 13, 16, 17, 18, 20), the AAE score is high or the performance gain of gaze prediction is lim-

Method	AAE (deg)	AUC
Huang <i>et al.</i> [11]	6.264	0.910
DFG [54]	6.301	0.923
Our full MCN (wrong)	5.910	0.927
Our full MCN (correct)	5.621	0.934

Table 3. Comparison of gaze prediction performance on EGTEA dataset. We place the results of previous gaze prediction method on the first two rows. On the last two rows, we split our result into two groups: *Our full MCN (wrong)* denotes the performance of our MCN when action recognition is wrong, and *Our full MCN (correct)* is the gaze prediction performance when action recognition is correct. Lower AAE and higher AUC indicate better performance. Our full MCN outperforms previous methods even with wrong action recognition.

Clip Acc. (%)	Top1	Top3	Top5
Ours MCN	51.42	73.64	81.94

Table 4. Top1, top3 and top5 action recognition accuracy of our method. The top3 accuracy is the fraction of testing set where the ground-truth label is among the three most probable classes from the model’s prediction. Top5 accuracy is defined accordingly.

ited. However, no performance degradation has been seen except for action 13. The result reveals that our method is robust to imperfect action recognition.

For further analysis, we split the gaze prediction performance into two groups: *Our full MCN (wrong)* is the gaze prediction result when the action recognition module fails, and *Our full MCN (correct)* is the result when the action recognition module successes. Table 3 lists the gaze prediction performance of our method and two state of the art gaze prediction methods. Although gaze prediction performance of our MCN degrades slightly when action recognition fails, the performance is still better than previous gaze prediction methods [11, 54]. We think that although action recognition fails in *Our full MCN (wrong)*, the action-based gaze prediction module can still take advantage of the action-based information from the input action likelihood. As shown in Table 4, the top3 and top5 accuracy are significantly higher than the top1 accuracy. The result indicates that even though the action recognition might fail, the ground-truth action label still remains a relatively high influence in the predicted action likelihood.

5. Conclusion and future work

In this work, we proposed a novel deep model for both egocentric gaze prediction and action recognition. Our model explicitly leverages the mutual context between the two tasks and achieves state of the art performance in both tasks on a public egocentric video dataset. Although our model can reliably predict gaze within an action period

compared with previous methods, gaze prediction performance still needs further improvement, especially for the transition moment between consecutive actions. We think it would be interesting future work to explore the gaze transition patterns relevant to the performed actions.

References

- [1] A. Betancourt, P. Morerio, C. S. Regazzoni, and M. Rauterberg. The evolution of first person vision methods: A survey. *IEEE Transactions on Circuits and Systems for Video Technology*, 25(5):744–760, 2015. 1
- [2] A. Borji, H. R. Tavakoli, D. N. Sihite, and L. Itti. Analysis of scores, datasets, and models in visual saliency prediction. In *Proceedings of the IEEE international conference on computer vision*, pages 921–928, 2013. 5
- [3] J. Carreira and A. Zisserman. Quo vadis, action recognition? a new model and the kinetics dataset. In *Computer Vision and Pattern Recognition (CVPR), 2017 IEEE Conference on*, pages 4724–4733. IEEE, 2017. 3, 4, 5, 6, 7
- [4] D. Chen, L. Yuan, J. Liao, N. Yu, and G. Hua. Stylebank: An explicit representation for neural image style transfer. In *2017 IEEE Conference on Computer Vision and Pattern Recognition (CVPR)*, pages 2770–2779. IEEE, 2017. 4
- [5] A. Fathi, A. Farhadi, and J. M. Rehg. Understanding egocentric activities. In *Computer Vision (ICCV), 2011 IEEE International Conference on*, pages 407–414. IEEE, 2011. 2
- [6] A. Fathi, Y. Li, and J. M. Rehg. Learning to recognize daily actions using gaze. In *ECCV*, 2012. 1, 2, 4
- [7] M. Fujisaki, H. Takenouchi, and M. Tokumaru. Interactive evolutionary computation using multiple users gaze information. In *International Conference on Human-Computer Interaction*, pages 109–116. Springer, 2017. 2
- [8] J. Harel, C. Koch, and P. Perona. Graph-based visual saliency. In *Advances in neural information processing systems*, pages 545–552, 2007. 5, 6
- [9] X. Huang, C. Shen, X. Boix, and Q. Zhao. Salicon: Reducing the semantic gap in saliency prediction by adapting deep neural networks. In *Proceedings of the IEEE International Conference on Computer Vision*, pages 262–270, 2015. 3, 6
- [10] Y. Huang, M. Cai, H. Kera, R. Yonetani, K. Higuchi, and Y. Sato. Temporal localization and spatial segmentation of joint attention in multiple first-person videos. In *Computer Vision Workshop (ICCVW), 2017 IEEE International Conference on*, pages 2313–2321. IEEE, 2017. 2
- [11] Y. Huang, M. Cai, Z. Li, and Y. Sato. Predicting gaze in egocentric video by learning task-dependent attention transition. In *ECCV*, 2018. 1, 2, 3, 4, 6, 9, 10
- [12] L. Itti and C. Koch. A saliency-based search mechanism for overt and covert shifts of visual attention. *Vision research*, 40(10-12):1489–1506, 2000. 5, 6
- [13] W. Kay, J. Carreira, K. Simonyan, B. Zhang, C. Hillier, S. Vijayanarasimhan, F. Viola, T. Green, T. Back, P. Natsev, et al. The kinetics human action video dataset. *arXiv preprint arXiv:1705.06950*, 2017. 5
- [14] H. Kera, R. Yonetani, K. Higuchi, and Y. Sato. Discovering objects of joint attention via first-person sensing. In *Proceed-*

- ings of the *IEEE Conference on Computer Vision and Pattern Recognition Workshops*, pages 7–15, 2016. 2
- [15] M. Khamis, F. Alt, M. Hassib, E. von Zezschwitz, R. Hasholzner, and A. Bulling. Gazetouchpass: Multimodal authentication using gaze and touch on mobile devices. In *Proceedings of the 2016 CHI Conference Extended Abstracts on Human Factors in Computing Systems*, pages 2156–2164. ACM, 2016. 2
- [16] D. P. Kingma and J. Ba. Adam: A method for stochastic optimization. *arXiv preprint arXiv:1412.6980*, 2014. 5
- [17] K. M. Kitani, T. Okabe, Y. Sato, and A. Sugimoto. Fast unsupervised ego-action learning for first-person sports videos. In *Computer Vision and Pattern Recognition (CVPR), 2011 IEEE Conference on*, pages 3241–3248. IEEE, 2011. 2
- [18] J. Kopf, M. F. Cohen, and R. Szeliski. First-person hyperlapse videos. *ACM Transactions on Graphics (TOG)*, 33(4):78, 2014. 1
- [19] A. Kurauchi, W. Feng, A. Joshi, C. Morimoto, and M. Betke. Eyeswipe: Dwell-free text entry using gaze paths. In *Proceedings of the 2016 CHI Conference on Human Factors in Computing Systems*, pages 1952–1956. ACM, 2016. 2
- [20] G. Li and Y. Yu. Visual saliency based on multiscale deep features. In *Proceedings of the IEEE conference on computer vision and pattern recognition*, pages 5455–5463, 2015. 3
- [21] Y. Li, A. Fathi, and J. M. Rehg. Learning to predict gaze in egocentric video. In *ICCV*, 2013. 1, 2, 4
- [22] Y. Li, M. Liu, and J. M. Rehg. In the eye of beholder: Joint learning of gaze and actions in first person video. In *ECCV*, 2018. 1, 2, 4, 5, 6, 7
- [23] Y. Li, Z. Ye, and J. M. Rehg. Delving into egocentric actions. In *IEEE Conference on Computer Vision and Pattern Recognition (CVPR)*, pages 287–295. IEEE, 2015. 1, 2, 5, 6, 7
- [24] Z. Lu and K. Grauman. Story-driven summarization for egocentric video. In *IEEE Conference on Computer Vision and Pattern Recognition*, pages 2714–2721. IEEE, 2013. 1
- [25] M. Ma, H. Fan, and K. M. Kitani. Going deeper into first-person activity recognition. In *Proceedings of the IEEE Conference on Computer Vision and Pattern Recognition*, pages 1894–1903, 2016. 1, 2
- [26] T. McCandless and K. Grauman. Object-centric spatio-temporal pyramids for egocentric activity recognition. In *BMVC*, volume 2, page 3. Citeseer, 2013. 2
- [27] K. Ogaki, K. M. Kitani, Y. Sugano, and Y. Sato. Coupling eye-motion and ego-motion features for first-person activity recognition. In *Computer Vision and Pattern Recognition Workshops (CVPRW), 2012 IEEE Computer Society Conference on*, pages 1–7. IEEE, 2012. 2
- [28] J. Pan, C. C. Ferrer, K. McGuinness, N. E. O’Connor, J. Torres, E. Sayrol, and X. Giro-i Nieto. Salgan: Visual saliency prediction with generative adversarial networks. *arXiv preprint arXiv:1701.01081*, 2017. 3
- [29] H. S. Park, E. Jain, and Y. Sheikh. 3d social saliency from head-mounted cameras. In *Advances in Neural Information Processing Systems*, pages 422–430, 2012. 2
- [30] D. Parkhurst, K. Law, and E. Niebur. Modeling the role of salience in the allocation of overt visual attention. *Vision research*, 42(1):107–123, 2002. 2
- [31] A. Paszke, S. Gross, S. Chintala, G. Chanan, E. Yang, Z. DeVito, Z. Lin, A. Desmaison, L. Antiga, and A. Lerer. Automatic differentiation in pytorch. 2017. 5
- [32] H. Pirsivash and D. Ramanan. Detecting activities of daily living in first-person camera views. In *Computer Vision and Pattern Recognition (CVPR), 2012 IEEE Conference on*, pages 2847–2854. IEEE, 2012. 2
- [33] Y. Poley, A. Ephrat, S. Peleg, and C. Arora. Compact cnn for indexing egocentric videos. In *Applications of Computer Vision (WACV), 2016 IEEE Winter Conference on*, pages 1–9. IEEE, 2016. 2
- [34] Y. Poley, T. Halperin, C. Arora, and S. Peleg. Egosampling: Fast-forward and stereo for egocentric videos. In *Proceedings of the IEEE Conference on Computer Vision and Pattern Recognition*, pages 4768–4776, 2015. 1
- [35] N. Riche, M. Duvinage, M. Mancas, B. Gosselin, and T. Du-toit. Saliency and human fixations: state-of-the-art and study of comparison metrics. In *Proceedings of the IEEE international conference on computer vision*, pages 1153–1160, 2013. 5
- [36] M. S. Ryoo, B. Rothrock, and L. Matthies. Pooled motion features for first-person videos. In *Proceedings of the IEEE Conference on Computer Vision and Pattern Recognition*, pages 896–904, 2015. 2
- [37] Y. Shen, B. Ni, Z. Li, and N. Zhuang. Egocentric activity prediction via event modulated attention. In *Proceedings of the European Conference on Computer Vision (ECCV)*, pages 197–212, 2018. 2
- [38] K. Simonyan and A. Zisserman. Two-stream convolutional networks for action recognition in videos. In *Advances in neural information processing systems*, pages 568–576, 2014. 3
- [39] S. Singh, C. Arora, and C. Jawahar. First person action recognition using deep learned descriptors. In *Proceedings of the IEEE Conference on Computer Vision and Pattern Recognition*, pages 2620–2628, 2016. 2, 6, 7
- [40] S. Song, C. Lan, J. Xing, W. Zeng, and J. Liu. An end-to-end spatio-temporal attention model for human action recognition from skeleton data. In *AAAI*, volume 1, pages 4263–4270, 2017. 3
- [41] E. H. Spriggs, F. De La Torre, and M. Hebert. Temporal segmentation and activity classification from first-person sensing. In *Computer Vision and Pattern Recognition Workshops, 2009. CVPR Workshops 2009. IEEE Computer Society Conference On*, pages 17–24. IEEE, 2009. 2
- [42] D. Surie, T. Pederson, F. Lagriffoul, L.-E. Janlert, and D. Sjölie. Activity recognition using an egocentric perspective of everyday objects. In *International Conference on Ubiquitous Intelligence and Computing*, pages 246–257. Springer, 2007. 2
- [43] S. P. Tipper, C. Lortie, and G. C. Baylis. Selective reaching: evidence for action-centered attention. *Journal of Experimental Psychology: Human Perception and Performance*, 18(4):891, 1992. 1
- [44] G. Varol, I. Laptev, and C. Schmid. Long-term temporal convolutions for action recognition. *IEEE transactions on pattern analysis and machine intelligence*, 40(6):1510–1517, 2018. 3

- [45] J. N. Vickers. Advances in coupling perception and action: the quiet eye as a bidirectional link between gaze, attention, and action. *Progress in brain research*, 174:279–288, 2009. [1](#)
- [46] H. Wang, A. Kläser, C. Schmid, and C.-L. Liu. Action recognition by dense trajectories. In *Computer Vision and Pattern Recognition (CVPR), 2011 IEEE Conference on*, pages 3169–3176. IEEE, 2011. [7](#)
- [47] L. Wang, H. Lu, X. Ruan, and M.-H. Yang. Deep networks for saliency detection via local estimation and global search. In *Proceedings of the IEEE Conference on Computer Vision and Pattern Recognition*, pages 3183–3192, 2015. [3](#)
- [48] L. Wang, Y. Xiong, Z. Wang, Y. Qiao, D. Lin, X. Tang, and L. Van Gool. Temporal segment networks: Towards good practices for deep action recognition. In *European Conference on Computer Vision*, pages 20–36. Springer, 2016. [3](#)
- [49] J. Xu, L. Mukherjee, Y. Li, J. Warner, J. M. Rehg, and V. Singh. Gaze-enabled egocentric video summarization via constrained submodular maximization. In *Proceedings of the IEEE Conference on Computer Vision and Pattern Recognition*, pages 2235–2244, 2015. [1](#), [2](#)
- [50] T. Xue, J. Wu, K. L. Bouman, and W. T. Freeman. Visual dynamics: Stochastic future generation via layered cross convolutional networks. In *IEEE Transactions on Pattern Analysis and Machine Intelligence (TPAMI)*, 2018. [4](#)
- [51] K. Yamada, Y. Sugano, T. Okabe, Y. Sato, A. Sugimoto, and K. Hiraki. Can saliency map models predict human egocentric visual attention? In *Asian Conference on Computer Vision*, pages 420–429. Springer, 2010. [2](#)
- [52] K. Yamada, Y. Sugano, T. Okabe, Y. Sato, A. Sugimoto, and K. Hiraki. Attention prediction in egocentric video using motion and visual saliency. In *Pacific-Rim Symposium on Image and Video Technology*, pages 277–288. Springer, 2011. [2](#)
- [53] R. Yonetani, K. M. Kitani, and Y. Sato. Recognizing micro-actions and reactions from paired egocentric videos. In *Proceedings of the IEEE Conference on Computer Vision and Pattern Recognition*, pages 2629–2638, 2016. [2](#)
- [54] M. Zhang, K. Teck Ma, J. Hwee Lim, Q. Zhao, and J. Feng. Anticipating where people will look using adversarial networks. In *IEEE Transactions on Pattern Analysis and Machine Intelligence (TPAMI)*, 2018. [1](#), [2](#), [3](#), [4](#), [6](#), [10](#)
- [55] R. Zhao, W. Ouyang, H. Li, and X. Wang. Saliency detection by multi-context deep learning. In *Proceedings of the IEEE Conference on Computer Vision and Pattern Recognition*, pages 1265–1274, 2015. [3](#)